

## On the Effects of kinetic minority ions on transport in Wendelstein 7-X

F. Schluck<sup>1</sup>, M. Rack<sup>1</sup>, Y. Feng<sup>2</sup>

<sup>1</sup>*Forschungszentrum Jülich GmbH, Institut für Energie- und Klimaforschung – Plasmaphysik,  
Partner of the Trilateral Euregio Cluster (TEC), 52425 Jülich, Germany*

<sup>2</sup>*Max-Planck-Institute für Plasmaphysik, 17491 Greifswald / 85748 Garching, Germany*

### Introduction

Since the early days of fusion research it is clear that the widely used fluid description has limited validity at least for partially charged particles. If thermalization processes are slow compared to e.g. ionization and recombination times or transport time scales, applying the overall more accurate kinetic treatment becomes mandatory. This may be the case in areas of low density, i.e. low collision frequency, or for ions that change their charge state or even return to plasma-facing components shortly after their birth.

Early work [1, 2] has e.g. stressed that partially charged carbon  $C^+ - C^{3+}$  under typical medium sized tokamak L-mode conditions requires a kinetic description. Recent studies [3] on helium plasmas in Wendelstein 7-X in limiter configuration have further underlined some weaknesses of a fluid treatment of  $He^+$ .

The kinetic Monte-Carlo code EIRENE [4] can be used for describing neutral particles in the plasma boundary of fusion devices. Coupling to the edge Monte-Carlo fluid code EMC3 has provided a code package capable of full three-dimensional investigations of plasma-wall interactions [5]. Traditionally, EIRENE has the option to follow motion of charged particles as well, but, although including effects like ionization, recombination, and thermal relaxation, tracing a very naive trajectory along the  $\mathbf{B}$ -field only. Recently, this model is being extended to include drift effects. This paper presents the implementation process including both technical and physical aspects.

### Code Fundament

Both codes, EIRENE and EMC3 are trajectory-based Monte-Carlo codes and are fully parallelized since long. This implies that in EIRENE (EMC3) the trajectory of single non-interacting test particles (fluid parcels) is traced and statistically evaluated to obtain parameters like impurity flow and plasma temperature, density, and momentum. Iteratively, test particles (fluid parcels) react on changed background conditions and, thus, the nonlinearities in the system are fully captured. The two codes work in similar ways, and a natural communication set-up for exchanging physics information is currently further modernized and upgraded [6].

EIRENE provides access to the incorporated physics through an interface, which allows rather straightforward coupling to fluid codes, e.g. B2.5 (SOLPS-ITER) [7], SOLEDGE2D [8], EMC3 etc., which typically require specific geometry options. For example, with EMC3, detailed grid information is only available on the fluid code side, which provides a rather tight monolithic coupling. To maintain this current flexibility in coupling requires additional effort in programming, as e.g. hard-coded drifts might be inappropriate in combination with a fluid code.

Readying EIRENE for refined kinetic ion treatment is not a new activity [9]. However, it turned out that the previous works cannot be simply adapted to the general 3D field geometry of the EMC3-EIRENE code package.

In the EMC3-EIRENE framework, intersection points and flight times between cells are calculated on the fluid side. Here, EMC3 sets the direction of the straight velocity to reach an intersection, which, in case of an unobstructed motion, is then used in EIRENE to update the particle location, although the correct physical velocity is not along that trajectory. Fig. 1 shows how an (unobstructed) trajectory is obtained in one cell in EMC3: The thick red arrow shows the real (guiding center averaged) trajectory from point A to B that an ion would undergo in that cell, regarding drifts. If the latter were disregarded, a charged particle would just follow the thin red arrow. Grid cells in EMC3 are aligned parallel to the magnetic field lines  $\mathbf{B}$ , which is why a particle starting at the surface  $(l_0, \varphi_0, m_0)$  in local coordinates along flux-tubes will hit the next boundary at  $(l_0, \varphi_0 + \Delta\varphi, m_0)$ . This local coordinate system is handy e.g. in the case of simulating plasmas in Wendelstein 7-X or (magnetically) perturbed tokamaks. If drifts are regarded, other geometrical parameters might change as well, as is e.g. shown in Fig. 1, where curvature-drift causes a change  $\Delta l$  in height.

So far, EIRENE cannot handle curved trajectories in the EMC3 geometry. The velocity vector used for pushing charged kinetic particles in EIRENE consists of two components: The first thick blue arrow denotes for the unobstructed path across the cell, i.e. represents  $\mathbf{v}_{\parallel}$ , where the index  $\parallel$  means parallel to the magnetic field vector. The second blue arrow denotes the pure drift movement perpendicular to the magnetic field, which is the here presented newly added feature, including checks whether this drift motion step causes a cell change (in  $r$ ,  $\Phi$  or  $z$ ). Note that the local magnetic coordinate system  $(l, \varphi, m)$  used in Fig. 1 does not make up the EMC3-EIRENE grid, which is in cylindrical coordinates  $(r, \Phi, z)$  (see light-blue rectangles in Fig. 1), where consecutive grid nodes in toroidal direction lie along magnetic field lines. Adding the two velocities together, one obtains the numerical guiding center velocity  $\mathbf{v}_{\text{gc}} = \mathbf{v}_{\parallel} + \mathbf{v}_{\text{drift}}$ , which points from the starting point to the final point in a straight line. At this final destination

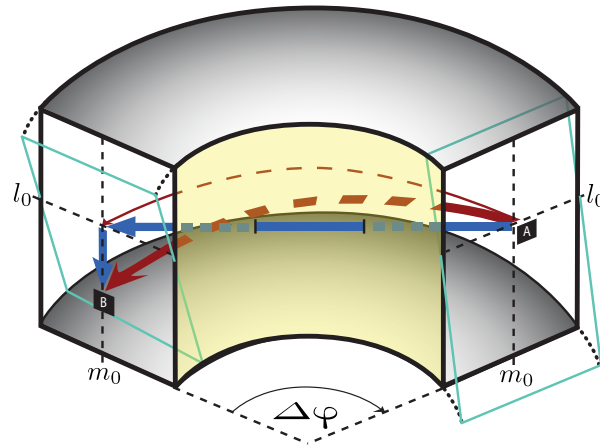


**Figure 1:** Ion (guiding center) trajectory (thick red) from point A to B on distinct surfaces in an EMC3 cell. The blue arrows represent EIRENE velocities  $\mathbf{v}_{\parallel}$  and  $\mathbf{v}_{\text{drift}}$ , whereas the latter is solely along the intersecting surface. Summation of the two velocities results in the guiding center velocity  $\mathbf{v}_{\text{gc}} = \mathbf{v}_{\parallel} + \mathbf{v}_{\text{drift}}$ . The approximated guiding center velocity  $\mathbf{v}_{\text{gc}}$  might intersect a neighboring cell (yellow surface), which can result in errors. Note that the pictured cell curvature is massively overdone for illustrative reasons.

both magnitude and direction of the new velocity are correct.

As is hinted in Fig. 1, this reduced trajectory following  $\mathbf{v}_{\text{gc}}$  might imply an intersection with a neighboring cell (blue arrow intersecting yellow surface). Particles undergoing such cell transitions may cause computational problems, which result in small, most time negligible discretization errors in particle balance, energy flux et cetera. Helium simulations exhibit larger errors because of the increased lifetime of  $\text{He}^+$  in comparison to  $\text{H}_2^+$  until destruction, i.e. a quotient of ionization times of  $\tau_{\text{H}_2^+}/\tau_{\text{He}^+} \approx 0.01$  for  $T_e \approx 20$  eV at densities around  $n_e = 10^{12} - 10^{14}$   $\text{cm}^{-3}$  [10].

The guiding center velocity is then returned to EIRENE which, depending on the path length in that cell, might perform reactions with the test particle which could prevent it from hitting the next grid surface.

So far, the code interface is set up to handle first order drift effects, i.e.  $\mathbf{E} \times \mathbf{B}$ -,  $\nabla|\mathbf{B}|$ -, and curvature-drift, where the two latter can be summarized into one equation (see Eq. (1)). The necessary gradient of the magnitude of the magnetic field is obtained via a simple cartesian stencil interpolation (on EMC3 side) in the interface (*vecusr* routine). This gradient is self-consistently and intrinsically calculated.

However, accounting for the former drift effect requires the electric field. Although the interface is completely set for calculating the  $\mathbf{E} \times \mathbf{B}$ -drift, so far the code package only accepts hard-coded or externally supplied electric fields. The proper calculation of the self-consistent electrostatic potential is, however, subject of current studies by Y. Feng [11] and therefore not covered here.

## First Order Drift Effects

The implemented drift effects [12] summarize in

$$\mathbf{v}_{\text{drift}} = \frac{\mathbf{E} \times \mathbf{B}}{B^2} + \frac{v_{\parallel}^2 + v_{\perp}^2/2}{q_j B/m_j} \frac{\mathbf{B} \times \nabla B}{B^2}, \quad (1)$$

where  $\mathbf{E}$  denotes the electric field,  $B$  is the absolute value of the magnetic field  $\mathbf{B}$ ,  $v_{\parallel}$  and  $v_{\perp}$  are the velocity components parallel and perpendicular to the magnetic field, respectively,  $q_j$  is the ion charge, and  $m_j$  the ion mass.

## Conclusion and Outlook

We introduced and explained in detail the implemented features of first order drift effects in the EMC3-EIRENE framework and discussed their shortcomings. With this, both hydrogen and helium simulations of Wendelstein 7-X in limiter configuration will be analyzed (see poster to this proceeding), which will be subject of ongoing research. It is foreseen to use the newly written routines in order to obtain the electric field [11] and run EMC3-EIRENE simulations for ITER as well.

## Acknowledgement

We thank D. Reiter for fruitful discussions. This work has been carried out within the framework of the EUROfusion Consortium and has received funding from the Euratom research and training programme 2014-2018 under grant agreement No 633053. The views and opinions expressed herein do not necessarily reflect those of the European Commission.

## References

- [1] P. Stangeby *et al.* **Computer Physics Communication** 28, (1988).
- [2] D. Reiser *et al.* **Nuclear Fusion** 2, 165-177, 38 (1998).
- [3] M. Rack *et al.* **Nuclear Fusion** 57, 056011 (2017).
- [4] EIRENE. <http://www.eirene.de>.
- [5] Y. Feng *et al.* **Journal of Nuclear Materials** 266-269, 812-818 (1999).
- [6] M. Rack *et al.* **EPS Conference Prague, conference contribution** (2018).
- [7] S. Wiesen *et al.* **Journal of Nuclear Materials** 463, 480-484 (2015)
- [8] H. Bufferand *et al.* **Nuclear Fusion** 55, 053025 (2015).
- [9] J. Seebacher and A. Kendl **Computer Physics Communication** 183, 947-959 (2012).
- [10] HYDKIN. <http://www.hydkin.de>.
- [11] Y. Feng **PSI Conference Princeton, conference contribution** (2018)..
- [12] J. Wesson **Tokamaks**, Oxford Science Publications, *Fourth Edition*, Ch. 2.6, p. 40ff, Eqs. (2.6.3), (2.6.9)